

## Study the Characteristics of Pionic Cascade Produced by Primary Proton in Extensive Air Showers

Shaimaa Rahem<sup>a</sup> , A. A. Al-Rubaiee<sup>b</sup>

Mustansiriyah University / College of Science , Department of Physics

<sup>a</sup>Shaimaarahem@uomustansiriyah.edu.iq , <sup>b</sup>dr.rubaiee@uomustansiriyah.edu.iq

### Abstract:

The study of high-energy cosmic rays represents one of the most challenging in the astroparticle physics field. A primary cosmic ray's interaction with the air atom's nucleus produces a huge number of secondary particles such as pions, electrons, neutrons, muons, etc. The Simulation of the Extensive Air Showers (EAS) at very high energies  $10^{19}$  and  $3 \times 10^{20}$  eV for primary proton was performed with the AIRES system (version 19.04.00) for vertical and inclined EAS showers. On the basis of this simulation, the effects of the EAS were described by the longitudinal development, lateral distribution function (LDF) and energy distribution at the ground respectively, for the pionic cascade produced by the primary proton. A new Gaussian function was obtained by approximating the longitudinal development for primary proton that produced charged pions as a function of the atmospheric depth of EAS showers, while a polynomial function was used for parameterization the described particle lateral density as function of the distance from the shower core and obtain a new parameters for primary proton. Moreover, a third order Polynomial equation used for energy distribution at ground as a function of the primary energies was estimated which is started in EAS, yielding four parameters for the primary proton. The comparison of the calculated longitudinal development, LDF, and energy distribution at the ground with that simulated with Scuitto has shown an opportunity for primary particle identification and definition of its energy at ultrahigh energies.

**Keywords:** Pionic cascade, Longitudinal development, Lateral distribution function, Energy distribution at the ground, AIRES system.

### دراسة خصائص البايونات

### الذي ينتجه البوتون الأولي في زخات الهواء الواسع

شيماء رحيم<sup>1,2</sup> , أحمد عزيز الربيعي<sup>2</sup>

<sup>1</sup>وزارة العلوم والتكنولوجيا

<sup>2</sup>قسم الفيزياء , كلية العلوم , الجامعة المستنصرية

### الخلاصة :

تمثل دراسة الأشعة الكونية عالية الطاقة واحدة من أكثر الدراسات تحدياً في مجال فيزياء الجسيمات الفلكية. ينتج تفاعل الشعاع الكوني الأولي مع نواة ذرة الهواء عدداً هائلاً من الجسيمات الثانوية مثل البايونات والإلكترونات والنيوترونات والميونات وما إلى ذلك. تم إجراء محاكاة زخات الهواء الواسعة (EAS) بطاقات عالية جداً ( $10^{19}$  و  $3 \times 10^{20}$  إلكترون فولت) للبوتون الأولي باستخدام نظام AIRES الإصدار (19.04.00) للاستحمام الرأسي والمائل من EAS على أساس هذه المحاكاة، تم وصف تأثيرات EAS من خلال التطوير الطولي ووظيفة التوزيع الجانبي (LDF) وتوزيع الطاقة على الأرض على التوالي، لوابل البايونات التي ينتجها البوتون الأولي. تم الحصول على وظيفة غاوسية جديدة عن طريق تقريب التطور الطولي للبوتون الأولي الذي أنتج البايونات المشحونة كدالة للعمق الجوي لزخات EAS، بينما تم استخدام وظيفة متعددة الحدود لتعيين الكثافة الجانبية للجسيمات الموصوفة كدالة للمسافة من قلب الدش والحصول على معلمات جديدة للبوتون الأولي. علاوة على ذلك، تم تقدير معادلة متعددة الحدود من الدرجة الثالثة المستخدمة لتوزيع الطاقة على الأرض كدالة للطاقات الأولية والتي بدأت في EAS، مما أسفر عن أربعة معلمات للبوتون الأولي. أظهرت مقارنة التطور الطولي المحسوب، LDF، وتوزيع الطاقة على الأرض مع تلك المحاكاة بواسطة (Scuitto) سكيوتو فرصة لتحديد الجسيمات الأولية وتعريف طاقتها في الطاقات فائقة.

## 1. Introduction

Ultra-High Energy Cosmic Rays (UHECRs) are the type of energetic particles that make up the majority of the universe's energetic dust. Studying the cascades that outcome from their nature interactions with atmospheric nuclei would yield many orders of magnitudes greater than results than those attained in artificial colliders and provide a rare understanding of the interaction characteristics of hadrons at center-of-mass energies [1]. When an atmospheric nucleus and UHECRs collide embarks on EAS of a nominated secondary particles accrual in the traversed air mass, which is commonly characterized to an incline depth,  $X$  [2]. Otherwise, EAS are a series of originated particles when a single primary cosmic ray with a high energy interacts with atmospheric nuclei made up of (Fe, He, C, and p), for example (O, N, and Ar). EAS expands in a intricate way by the generation of many particles from hadronic, muonic, and electromagnetic cascades [3, 4]. The EAS consists of different shower cascades. This can be classified into three cascades the electromagnetic, hadronic and muonic cascades. The EAS are known for about 70 years to be cascade started off by primary Cosmic Rays (CRs) in the atmosphere. Moreover, the EAS can be viewed as tools for astroparticle physics. The composition of the highest energy of the CRs is one of the most enigmatic phenomena in the universe. High-energy CRs have

been discovered through the originated EAS over the Earth's atmosphere. One of the extremely significant methods to study high energy of EAS is the longitudinal development, lateral distribution, and energy distribution at ground[5]. In 2005, a simple semi-empirical technique for improving the portion related to the hadronic air showers are analogous to the Heitler splitting manner has been used by J. Matthews. Furthermore, several merits of EAS are honestly demonstrated via numeral predictions in highly compatible data with a detailed simulation of Monte Carlo (MC). The reconstruction energy outcome, electron sizes, muon, and the effects of the atomic number of the primary were computed [4]. The lateral distribution function (LDF) is also extremely significant method to study high energy of EAS, it is the number of charged particles per unit of the detection area. The LDF related to charged particles over the EAS is the required amount to monitor Earth's CR, which is oftentimes concluded from the EAS results. Additionally, extra information is being exposed about astroparticle physics [6]. The reaction usually called a cascade carries on until the mean energy held by these single and multiple particles under their critical energies, which is frequently lost due to numerous collisions rather than other radiative methods [7]. So, it's ordinarily modeled via an MC simulation of every separate shower particle's interaction and transport, and rely on our modern comprehension of decays,

interactions, and particle transport inside matter [8]. As a result of the intricacy of the models engaged occur through the building of an air shower, numeral simulations are usually useful to carry out overall research of its characteristics. Therefore, the two simulations impact the interactions for particles and transport inside the atmosphere, also the system hypothesises, influence quantitative outcomes [9]. The total processes that possess a main effect on the shower's behaviors must be taken into consideration via the simulating algorithms. Also, all hadronic collisions, electrodynamic interactions, particle decays, photonuclear processes, and so on [10, 11]. As the standard technique to calculate air shower developments is the MC technique so in this paper we study the pionic cascade development produced

by the primary proton by simulating the longitudinal development, LDF, and energy distribution at the ground with two energies ( $10^{19}$ , and  $3 \times 10^{20}$ ) eV and two zenith angles  $0^\circ$  and  $30^\circ$ .

**2. Longitudinal profile of EAS**

The EAS longitudinal profile depicts the variation of shower particles number,  $N(X)$ , versus the overtime of the EAS develops[12]. In Fig.1, the line curve above the particle cascade illustrates the longitudinal cascade, also called the shower profile[13, 14]. Since the interactions in the shower depend on the atmospheric depth encountered via traveling shower particles, the number related to shower particles,  $N$ , is usually plotted against atmospheric depth [15]. The longitudinal cascade can be parameterized via the Gaisser-Hillas function[16]:

$$N(X) = N_{max} \left( \frac{X}{X_{max}} \right)^{X_{max}/\lambda} \exp \left( X_{max} - X \right) / \lambda \dots\dots\dots (1)$$

where,  $X$ , represents the atmospheric depth ( $g/cm^2$ );  $N_{max}$ , is maximum shower size, the maximum show-

er depth is represented by  $X_{max}$ , and  $\lambda$  represents the length parameter[17].

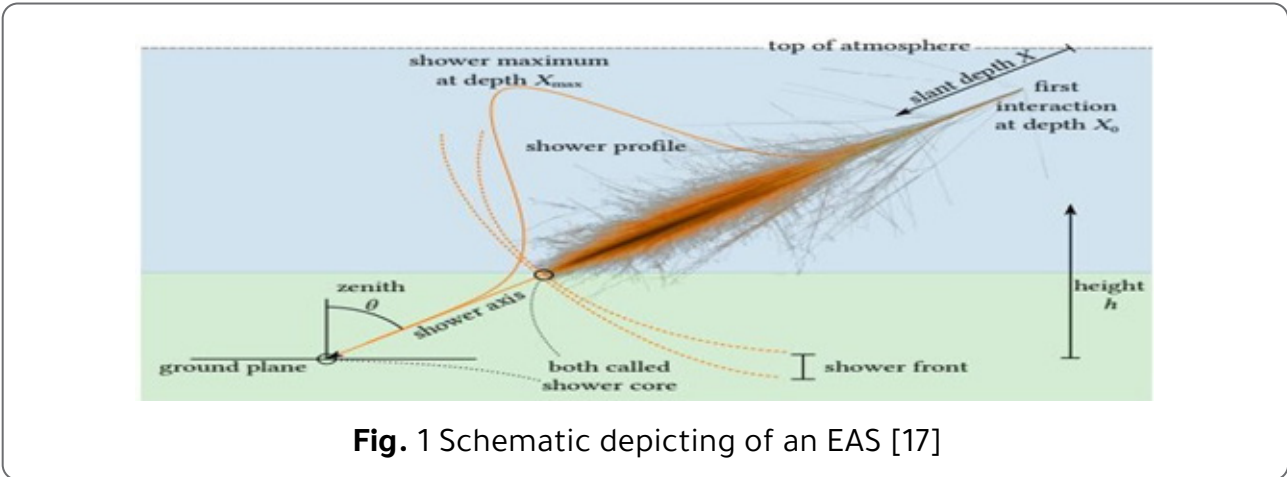


**Fig. 1** Schematic depicting of an EAS [17]

**2.2 Lateral distribution function**

Referring to the particle lateral density distribution related to EAS is a vital key part extreme of ground-based CRs experiments, the LDF represents a highly important factor in the description of the air-shower phenomenon [18]. The calculation of many scatterings related to Nishimura and Kamata inside the electromagnetic cascade of electrons was taken into consideration,

$$\rho\left(\frac{r}{R_M}, N_e, E_o, S\right) = \frac{N_e}{2\pi R_M^2} C(s) \left(\frac{r}{R_M}\right)^{(s-2)} \times \left(\frac{r}{R_M} + 1\right)^{(s-4.5)} \dots\dots\dots (2)$$

Where  $\rho(r)$  describes a particle density over a distance  $r$  started from the shower core and  $N_e$  represents the whole number of electrons inside the showers;  $R_M=118$  m is Molier radii;  $S$  is the shower age parameter, and  $C(s)$  is the normalizing factor of  $0.366 s^2 * (2.07 - s)^{1.25}$  [20]. Referring to the hadron launched showers characterized by NKG-like functions some researchers have aimed to get better fits by refining or adding the term for the lifetime parameter,  $S$  [ 21].

$$S = \frac{3}{1+(2\beta/t)} \dots\dots\dots(3)$$

Where  $\beta$  represents a free parameter and computes the variation between a pure electromagnetic shower and a hadron initiated air shower.

and the confirmed that the LDF relies on the lifetime (age )of the shower ( $s$ ). Moreover, the function of NKG is related to the distance from the core of the shower when divided over the Molier radius, primary energy, shower lifetime parameter, and shower size. Also, The NKG function is dependent on the whole number of electrons  $N_e$  at a specified depth, as described in the relationship [19]:

**2.3 Energy distribution at ground ( $E_{ground}$ )**

The hadronic component has been almost transformed to the other two components at ground level. The density of the secondary particles produced in the hadronic reaction is important in forming and the growth of the shower pions. Pions constitute the majority of the secondary particles generated with all species ( $\pi^0, \pi^-,$  and  $\pi^+$ ) produced in equal number see Figure (2) [22].

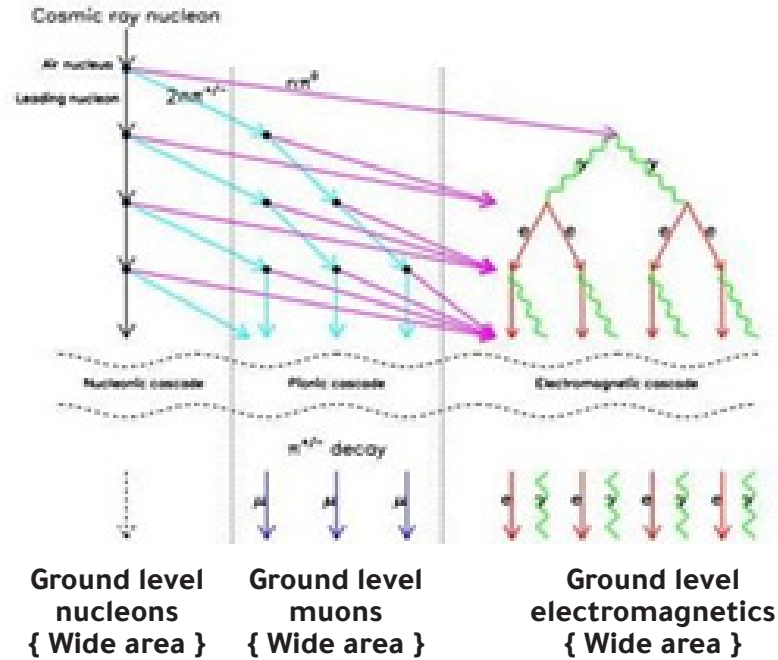


**Fig. 2 :** The hadronic component of the shower pions [22]

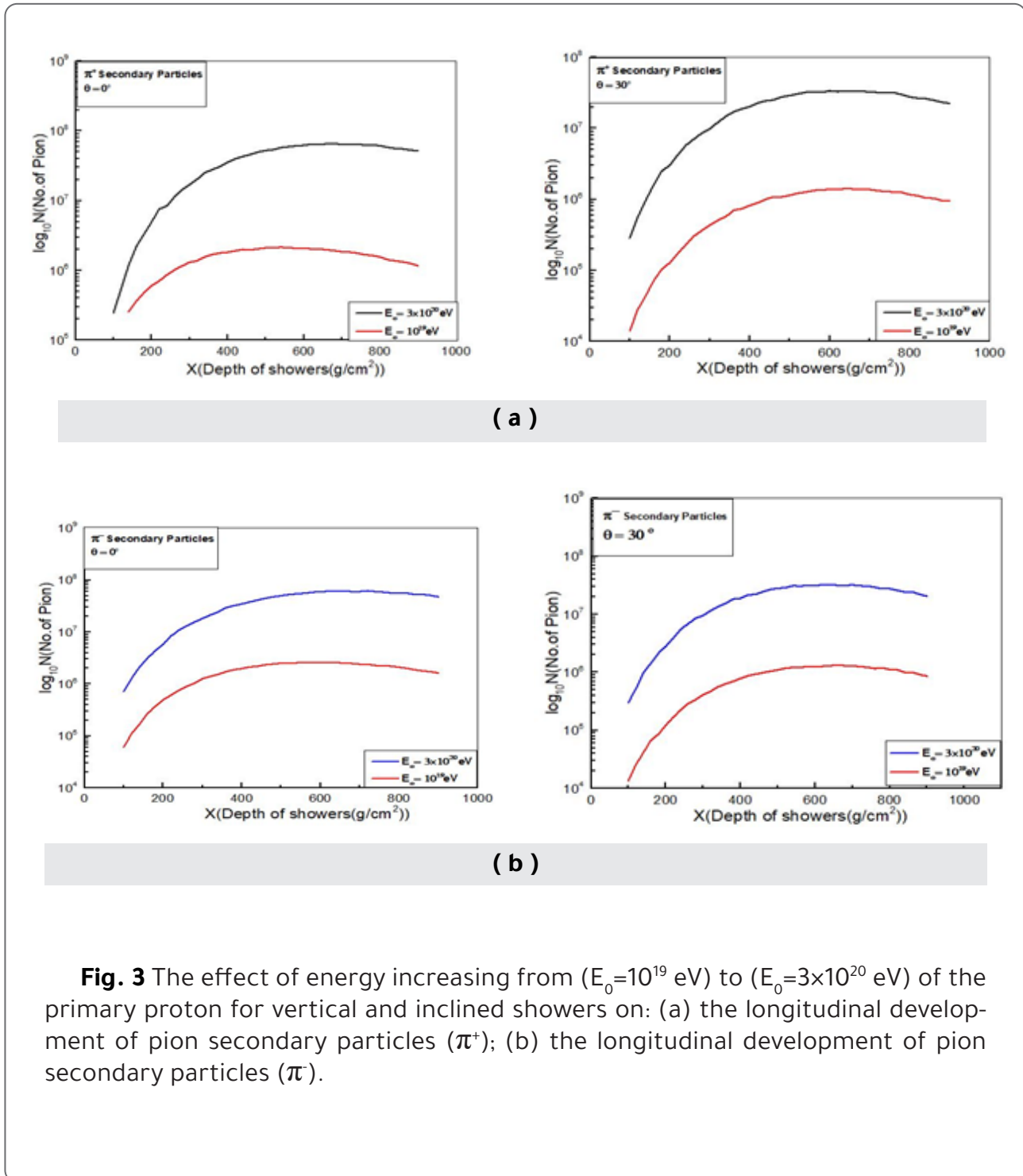
### 3. The Simulation using AIRES code

AIRES is an abbreviation for "AIR-shower Extended Simulations", it is a series of successive programs models and sequent subroutines that employed to simulate EAS particle cascades when the primary CRs interacts with high atmospheric energy, as well as the controlling of all associated data outputs[23]. AIREs simulates comprehensive space-time particle spread in a real surroundings with geomagnetic field, the atmosphere, and curvature of the earth is taken in consideration [24]. These simulations were performed for primary proton with two energies ( $10^{19}$ , and  $3 \times 10^{20}$ ), and two zenith angles ( $0^\circ$  and  $30^\circ$ ) us-

ing the high energy hadronic model Sibyll 2.3c with the thinning energy ( $\epsilon_{th}=10^{-7}$ ). Moreover, the longitudinal development, LDF, and the energy distribution at ground of the air shower carry important parameters for estimating the mass formation of the high-energy primary proton that strike the Earth's atmosphere by analyzing the number of charged pion secondary particles produced as a function of the (penetration depth inside the atmosphere, the energy distribution at ground, and the LDF) at ultrahigh energies. In Fig. 3 shown the simulation of the longitudinal development for primary proton and the effect of increased primary energy between  $10^{19}$  eV and  $3 \times 10^{20}$  eV for vertical and

inclined EAS showers. The results observed that, as the energy of incident primary proton increases, the pro-

duced number of secondary particles ( $\pi^+$  &  $\pi^-$ ) increases.



In Fig. 4 shown the simulation of LDF for primary proton for proton primary particles and the effect of energy increasing between  $10^{19}$  eV and  $3 \times 10^{20}$  eV for vertical and inclined EAS

showers. The results observed that, when the energy of incident primary proton increases, the produced number of secondary particles ( $\pi^+$  &  $\pi^-$ ) increases too.

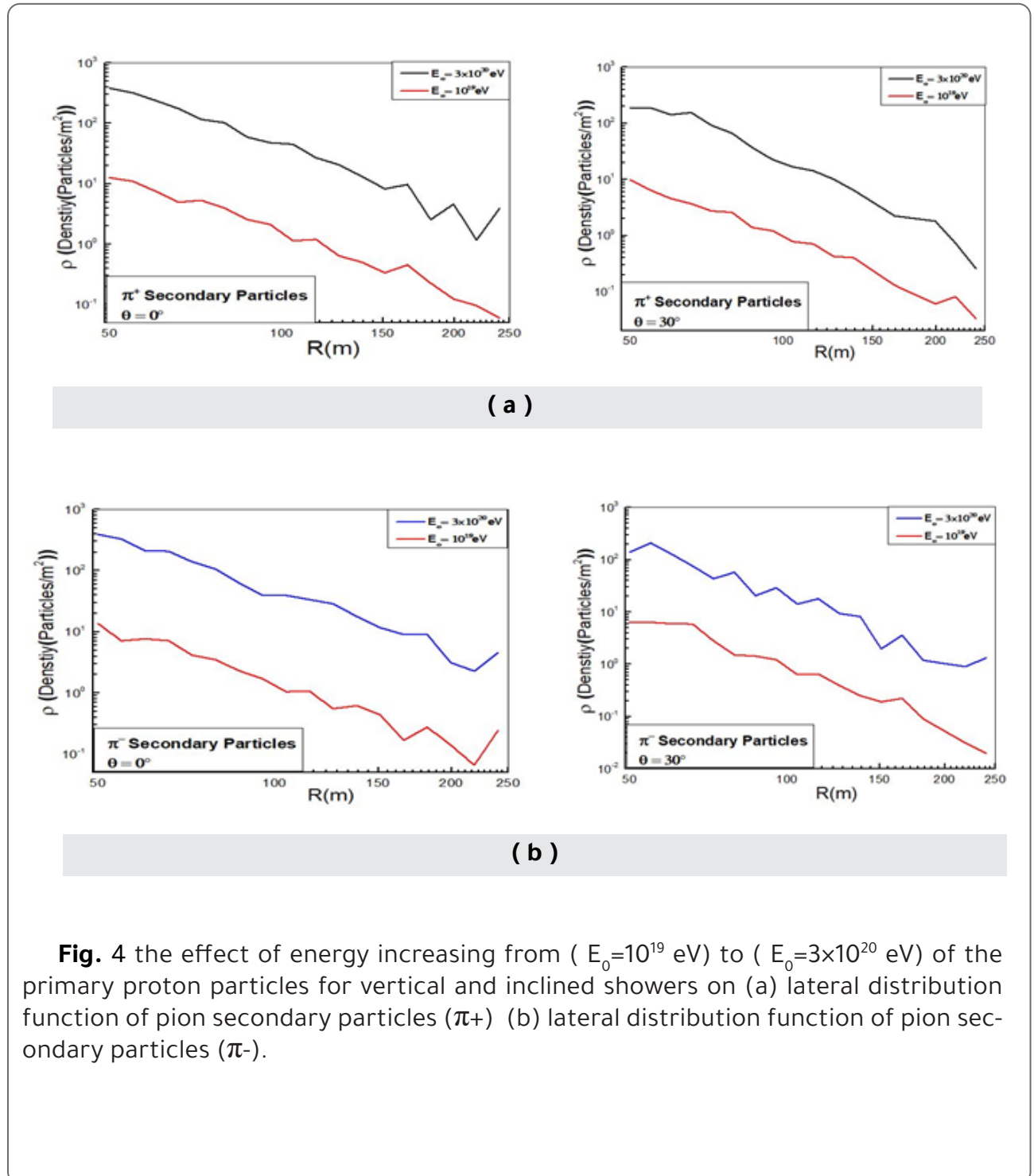
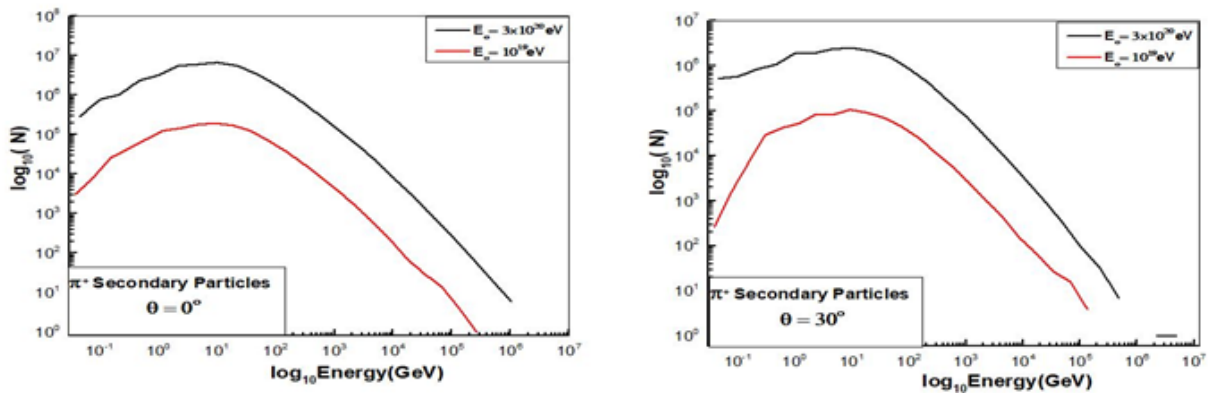


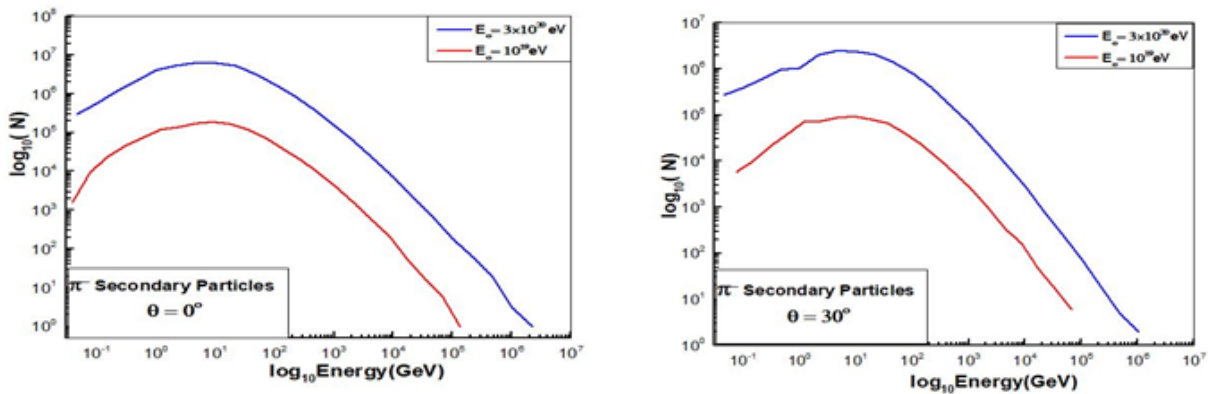
**Fig. 4** the effect of energy increasing from ( $E_0=10^{19}$  eV) to ( $E_0=3 \times 10^{20}$  eV) of the primary proton particles for vertical and inclined showers on (a) lateral distribution function of pion secondary particles ( $\pi^+$ ) (b) lateral distribution function of pion secondary particles ( $\pi^-$ ).

In Fig. 5 shown the simulation of energy distribution at ground ( $E_{ground}$ ) for proton primary particles and the impact of increased primary energy from  $10^{19}$  eV and  $3 \times 10^{20}$  eV for verti-

cal and inclined EAS showers. The results observed that, as the energy of incident primary proton increases, the produced number of secondary particles ( $\pi^+$  &  $\pi^-$ ) increases.



( a )



( b )

**Fig. 5** the effect of energy increasing from ( $E_0=10^{19}$  eV) to ( $E_0=3 \times 10^{20}$  eV) of the primary proton particles for vertical and inclined showers on (a) energy distribution at ground ( $E_{ground}$ ) of pion secondary particles ( $\pi^+$ ) (b) energy distribution at ground ( $E_{ground}$ ) of pion secondary particles ( $\pi^-$ ).

## 4. Results and Discussion

### 4.1 Longitudinal Development Parameterizations

The Aires simulation was utilized for the primary proton within two primary energies  $10^{19}$  and  $3 \times 10^{20}$  eV and scouted the longitudinal development for two

zenith angles  $0^\circ$  and  $30^\circ$ . A Gaussian function was applied to parameterize the longitudinal development of showers that begin in EAS, collecting four of important parameters for the primary proton, the function is designated by:

$$N_{\pi}(X) = \eta + (\alpha / (\omega * \sqrt{\pi / 2})) * e^{-2 * \left(\frac{X - X_c}{\omega}\right)^2} \dots \dots \dots (4)$$

Where,  $\eta, \alpha, \omega$  and  $X_c$  are Coefficients obtained from the Gaussian function for the longitudinal develop-

ment in EAS;  $N_{\pi}$  is the number of pions in the shower as a function of the shower depth ( $X$ ) as listed in Table 1.

**Table 1.** the Coefficients of Gaussain function (Eq. 4) for primary proton.

Primary particles	Secondary particles	Primary Energy (eV)	Coefficients $\theta = 0^\circ$				$R^2$
			$\eta$	$\alpha$	$\omega$	$\delta$	
p	$\pi^+$	$10^{19}$	$10^6 \times -1.429$	$10^9 \times 3.581$	696.197	618.610	0.992
		$10^{20} \times 3$	$10^7 \times -1.418$	$10^{10} \times 5.96$	618.409	691.894	0.996
	$\pi^-$	$10^{19}$	$10^6 \times -1.499$	$10^{10} \times 3.66$	708.233	616.043	0.992
		$10^{20} \times 3$	$10^6 \times -1.289$	$10^{10} \times 5.67$	604.140	689.686	0.996
Primary particles	Secondary particles	Primary Energy (eV)	Coefficients $\theta = 30^\circ$				$R^2$
			$\eta$	$\alpha$	$\omega$	$\delta$	
p	$\pi^+$	$10^{19}$	-236252.62	$10^9 \times 1.120$	543.570	657.706	0.996
		$10^{20} \times 3$	$10^6 \times -6.643$	$10^9 \times 2.824$	552.314	654.168	0.994
	$\pi^-$	$10^{19}$	-248177.51	$10^9 \times 1.095$	556.608	659.285	0.996
		$10^{20} \times 3$	-515845.22	$10^{10} \times 2.61$	541.904	653.652	0.995

The figure 6 display the parameterization of longitudinal development that simulated with AIREs system in EAS using the Gaussian function (Eq.

4) for the energies ( $10^{19}$  and  $3 \times 10^{20}$ ) eV with two zenith angles ( $0^\circ$  and  $30^\circ$ ) for pions secondary particles.

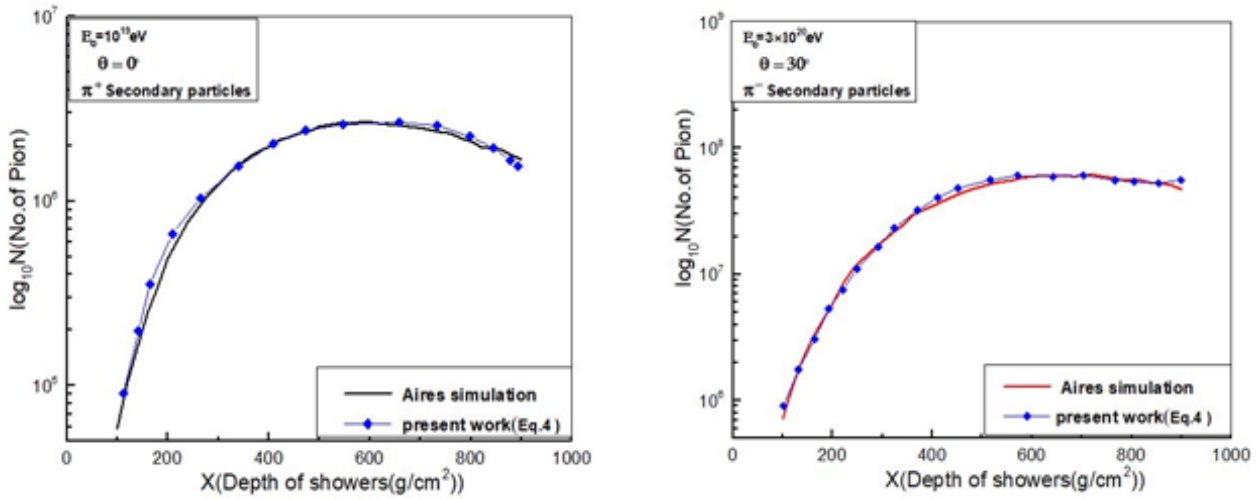


Fig. 6 Longitudinal development simulated using AIREs (solid lines) vs. one computed using (Eq.4) (dashed lines) for Primary proton.

**4.2 Lateral distribution function parameterizations**

The Aires simulation was employed for the primary proton within two primary energies  $10^{19}$  and  $3 \times 10^{20}$  eV and explores the lateral distribution for two

zenith angles  $0^\circ$  and  $30^\circ$ . A polynomial function was conducted to parameterize the lateral distribution of showers that originated in EAS, collecting four parameters for the primary proton, the function is designated by:

$$\rho(R) = B_0 + B_1R + B_2R^2 + B_3R^3 \dots\dots\dots (5)$$

Where,  $B_0, B_1, B_2$  and  $B_3$  are Coefficients obtained from the polynomial function for the lateral distribution in

EAS, shower density of pions as a function of the distance from the shower core as listed in Table 2.

**Table 2.** Coefficients of the polynomial function of (Eq. 5) for primary proton.

Primary particles	Secondary particles	Primary Energy (eV)	Coefficients $\theta = 0^\circ$				$R^2$
			$B_0$	$B_1$	$B_2$	$B_3$	
p	$\pi^+$	$10^{19}$	11.604	-12.654	5.713	-1.115	0.987
		$10^{20} \times 3$	-35.395	61.446	-31.761	5.147	0.956
	$\pi^-$	$10^{19}$	-60.258	97.430	-50.220	8.305	0.951
		$10^{20} \times 3$	-5.807	17.256	-9.985	1.613	0.970
Primary particles	Secondary particles	Primary Energy (eV)	Coefficients $\theta = 30^\circ$				$R^2$
			$B_0$	$B_1$	$B_2$	$B_3$	
p	$\pi^+$	$10^{19}$	8.045	-6.979	2.625	-0.573	0.987
		$10^{20} \times 3$	0.328	4.923	-2.161	-0.016	0.983
	$\pi^-$	$10^{19}$	14.732	-18.737	9.402	-1.859	0.980
		$10^{20} \times 3$	-50.393	83.479	-42.693	6.936	0.948

The figure 7 display the parameterization of the lateral distribution that simulated with AIREs system in EAS using the polynomial function (Eq. 5)

for the energies ( $1 \times 10^{19}$  and  $3 \times 10^{20}$ ) eV with both zenith angles ( $0^\circ$  and  $30^\circ$ ) for charged pions secondary particles.

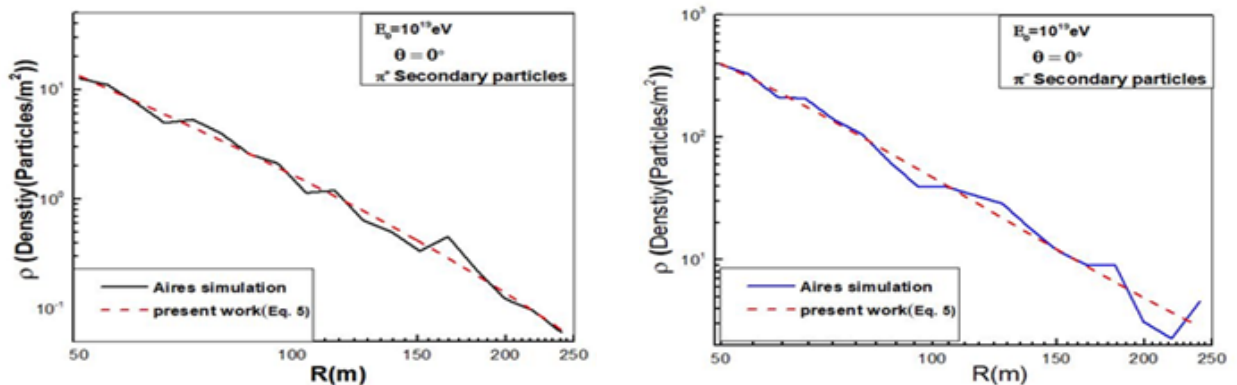


**Fig. 7** the lateral distribution simulated using AIREs (solid lines) vs. one computed using (Eq.5) (dashed lines) for Primary proton.

### 4.3 Parameterization of the energy distribution at ground

The Aires simulation was conducted for the primary proton within two primary energies  $10^{19}$  and  $3 \times 10^{20}$  eV and explores the energy distribution for two

zenith angles  $0^\circ$  and  $30^\circ$ . A polynomial function was employed to parameterize the energy distribution of showers that originated in EAS, collecting four parameters for the primary proton, the function is designated by:

$$N_\pi(E_{ground}) = C_0 + C_1 E_{ground} + C_2 E_{ground}^2 + C_3 E_{ground}^3 \dots\dots\dots (6)$$

Where,  $C_0, C_1, C_2$  and  $C_3$  are Coefficients obtained from the polynomial function for the energy distribution at ground in EAS, the energy distribu-

tion at ground of pions in the shower as a function of the primary energy as listed in Table 3.

**Table 3.** Coefficients of the polynomial function of (Eq. 6) for primary proton.

Primary particles	Secondary particles	Primary Energy (eV)	Coefficients $\theta = 0^\circ$				$R^2$
			$C_0$	$C_1$	$C_2$	$C_3$	
p	$\pi^+$	$10^{19}$	5.086	0.536	-0.416	0.027	0.998
		$10^{20} \times 3$	6.634	0.437	-0.362	0.021	0.998
	$\pi^-$	$10^{19}$	5.053	0.585	-0.415	0.022	0.998
		$10^{20} \times 3$	6.633	0.448	-0.368	0.021	0.998
Primary particles	Secondary particles	Primary Energy (eV)	Coefficients $\theta = 30^\circ$				$R^2$
			$C_0$	$C_1$	$C_2$	$C_3$	
p	$\pi^+$	$10^{19}$	3.2866	0.80634	-0.480	0.037	0.989
		$10^{20} \times 3$	6.40728	0.28594	-0.336	0.021	0.994
	$\pi^-$	$10^{19}$	4.79546	0.55139	-0.417	0.027	0.998
		$10^{20} \times 3$	6.28036	0.34566	-0.32689	0.016	0.994

The figure 8 display shows the parameterization of energy distribution at ground that simulated with AIRES system in EAS using the polynomial

function (Eq. 6) for the energies ( $1 \times 10^{19}$  and  $3 \times 10^{20}$ ) eV with two zenith angles ( $0^\circ$  and  $30^\circ$ ) for charged pions secondary particles.

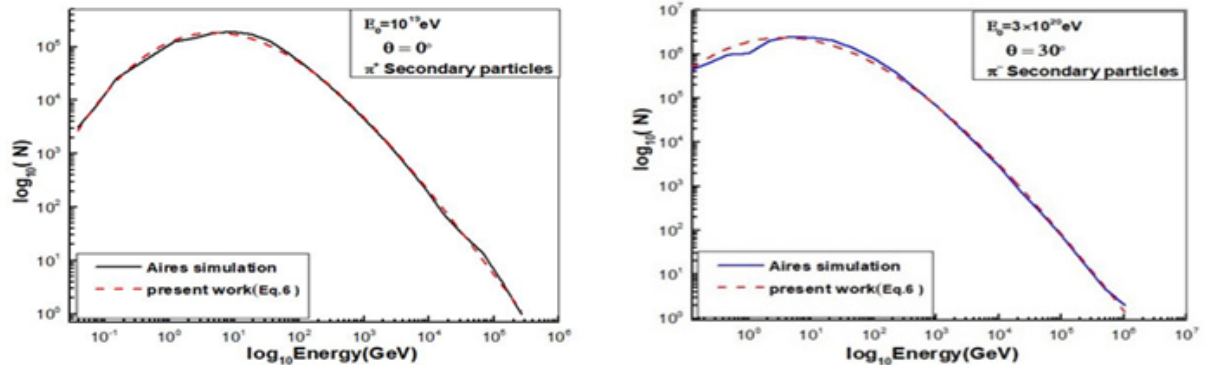


**Fig. 8** the energy distribution at ground simulated using AIRES (solid lines) vs. one computed via (Eq.6) (dashed lines) for Primary proton.

### 5. The Comparison with S. J. Sciutto Simulation

The parameterized longitudinal development that was computed via Eq.4 was compared with the data simulated by S. J. Sciutto [25]. This com-

parison gave good compatibility at the same energy of  $3 \times 10^{20}$  eV for the primary proton for zenith angle ( $0^\circ$ ) that produced the charged pion secondary particle was observed in Fig. 9.

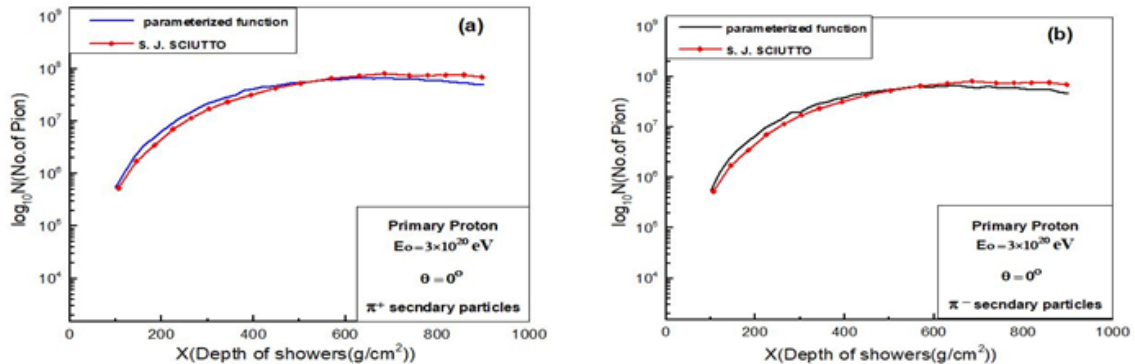


**Fig. 9** The comparison between the results obtained from the Eq.(4) and the data that simulated via S. J. Sciutto for the charged pion secondary particle ( (a)  $\pi^+$  and (b)  $\pi^-$  ) of the primary proton at the energy  $3 \times 10^{20}$  eV.

The parameterized lateral distribution and energy distribution at ground that was obtained using Eq.5 and Eq.6 was compared with the data simulated by S. J. Sciutto [25]. This comparison

gave good compatibility at the same energy of  $1 \times 10^{19}$  eV for the primary proton for zenith angle ( $0^\circ$ ) that produced the charged pion secondary particle was observed in Fig. 10.

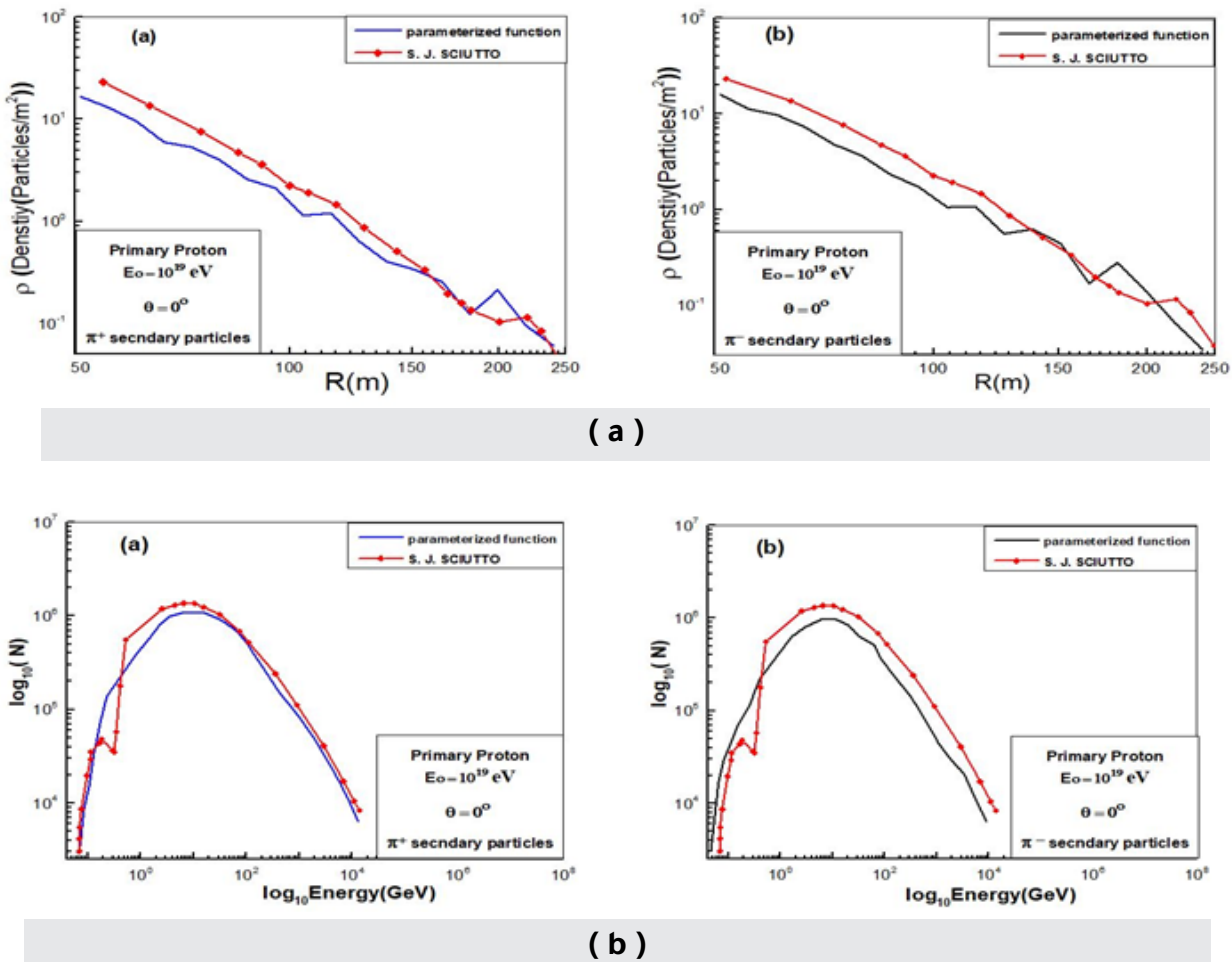


**Fig. 10** The comparison between the results obtained and the data that simulated via S. J. Sciuotto for the charged pion secondary particle ((A) lateral distribution ( (a)  $\pi^+$  , (b)  $\pi^-$  ) and (B) energy distribution at ground ( (a)  $\pi^+$  and (b)  $\pi^-$  ), of the primary proton at the energy  $1 \times 10^{19}$  eV.

### 6. Conclusions

The AIRES program was used to simulate the longitudinal development, lateral distribution and energy distribution at ground respectively, for primary proton at two energies ( $1 \times 10^{19}$  and  $3 \times 10^{20}$ ) eV with two zenith angles  $0^\circ$  and  $30^\circ$ . In the present work, it was noticed that the number of charged pion secondary particles that reach the Earth's surface is directly

proportional to the primary energy of incident particles. A new Gaussian function as a function of the penetration depth of EAS showers was parameterized for the simulated longitudinal development. These parameterized functions can be used to predicate the behavior of secondary particles. While the lateral distribution and energy distribution at ground using polynomial function gives new parameters for

proton primary particle. The comparison of the results parameterized with that simulated by Scuitto gave a good agreement in longitudinal development and energy distributions.

### References

- [1] A. Aab et al., "Probing the origin of ultra-high-energy cosmic rays with neutrinos in the EeV energy range using the Pierre Auger Observatory," *Journal of Cosmology and Astroparticle Physics*, vol. 2019, no. 10, p. 22, 2019.
- [2] A. Aab, "Pierre Auger Coll," *Nucl. Instrum. Meth. A*, vol. 798, pp. 172-213, 2015.
- [3] P. K. F. Grieder, "Extensive air showers. High energy phenomena and astrophysical aspects. Vol. 1 and 2. A tutorial, reference manual and data book," vol. 1, 11, 2010.
- [4] J. Matthews, "A Heitler model of extensive air showers," *Astroparticle Physics*, vol. 22, no. 5-6, pp. 387-397, 2005.
- [5] M. Risse, "Properties of extensive air showers," arXiv preprint [astro-ph/0402300](https://arxiv.org/abs/astro-ph/0402300), 2004.
- [6] A. Haungs, H. Rebel, and M. Roth, "Energy spectrum and mass composition of high-energy cosmic rays," *Reports on Progress in Physics*, vol. 66, no. 7, p. 1145, 2003.
- [7] S. P. Knurenko, A. A. Ivanov, M. I. Pravdin, A. V Sabourov, and I. Y. Sleptsov, "Recent results from Yakutsk experiment: development of EAS, energy spectrum and primary particle mass composition in the energy region of  $10^{15}$ - $10^{19}$  eV," arXiv preprint [astro-ph/0611871](https://arxiv.org/abs/astro-ph/0611871), 2006.
- [8] M. Roth, "The lateral distribution function of shower signals in the surface detector of the pierre auger observatory," arXiv preprint [astro-ph/0308392](https://arxiv.org/abs/astro-ph/0308392), 2003.
- [9] M. V. S. Rao and B. V. Sreekantan, *Extensive air showers*. World scientific, 1998.
- [10] S. J. Sciutto, "The AIREs system for air shower simulations. An update," *Proceedings of ICRC 2001 astro-ph/0106044*, 2001.
- [11] A. A. Al-Rubaiee and A. Jumaah, "Estimation of Lateral Distribution Function in Extensive Air Showers by Using AIREs Simulation System," arXiv preprint [arXiv:1305.4628](https://arxiv.org/abs/1305.4628), 2013.
- [12] A. Aab et al., "Reconstruction of events recorded with the surface detector of the Pierre Auger Observatory," *Journal of Instrumentation*, vol. 15, no. 10, p. P10021, 2020.
- [13] A. Aab et al., "Combined fit of spectrum and composition data as measured by the Pierre Auger Observatory," *Journal of Cosmology and Astroparticle Physics*, vol. 2017, no. 04, p. 38, 2017.
- [14] G. B. Gelmini, O. E. Kalashev, and D. V Semikoz, "GZK photons as ultra-high-energy cosmic rays," *Journal of Experimental and Theoretical Physics*, vol. 106, no. 6, pp. 1061-1082, 2008.
- [15] S. Bhatnagar, "Extensive Air Shower High Energy Cosmic Rays (II)," *Physics Education*, vol. 249, 2009.
- [16] A. R. Raham, A. A. Al-Rubaiee, and M. H. Al-Kubaisy, "Investigating the longitudinal development of EAS with ultra high energies," in *Journal of Physics: Conference Series*, 2020, vol. 1484, no. 1, p. 12024.
- [17] F. Riehn, H. P. Dembinski, R. Engel, A. Fedynitch, T. K. Gaisser, and T. Stanev, "The hadronic interaction model SIBYLL 2.3 c and Feynman scaling," *PoS*, vol. ICRC2017, p. 301, 2017.
- [18] S. J. Sciutto, "AIREs: A System for air shower simulations. User's guide and reference manual. Version 2.2. 0," 2019.
- [19] S. J. Sciutto, "AIREs: A system for air shower simulations," 1999, doi: "10.13140/RG.2.2.12566.40002."

- [20] K. F. Fadhel and A. A. Al-Rubaiee, "Simulation and parameterization of longitudinal development in extensive air showers for different hadronic interaction models," in AIP Conference Proceedings, 2022, vol. 2386, no. 1, p. 80044.
- [21] M. S. S. Mayotte, "Study of the Cosmic Ray Composition Sensitivity of AugerPrime," 2021.
- [22] T. K. Gaisser and A. M. Hillas, "Reliability of the method of constant intensity cuts for reconstructing the average development of vertical showers," in International Cosmic Ray Conference, 1977, vol. 8, p. 353.
- [23] J. Abraham et al., "Measurement of the depth of maximum of extensive air showers above  $10^{18}$  eV," Physical review letters, vol. 104, no. 9, p. 91101, 2010.
- [24] A. Tapia et al., "The lateral shower age parameter as an estimator of chemical composition," arXiv preprint arXiv:1309.3536, 2013.
- [25] J. Knapp, D. Heck, S. J. Sciutto, M. T. Dova, and M. Risse, "Extensive air shower simulations at the highest energies," Astroparticle Physics, vol. 19, no. 1, pp. 77-99, 2003.
- [26] O. A. M. A. H Kara, Extensive Air Showers High Energy Phenomena and Astrophysical Aspects, vol. 7, no. 2. 2014.
- [27] P. Hofverberg, "Air shower simulations for the SESA experiment, masters thesis," royal institute of technology, vol. department, 2003.
- [28] A. A. Al-Rubaiee and A. Jumaah, "Investigating of longitudinal development parameters through air shower simulation by different hadronic models," arXiv preprint arXiv:1309.2934, 2013.